Journal of
Applied Sciences

Mineralogical and Geochemical Characteristics of Clay Deposits from South Abarkouh District of Clay Deposit (Central Iran) and Their Applications

A.S. Mahjoor, M. Karimi and A. Rastegarlari

Department of Geology, Islamic Azad University of Shiraz, P.O. Box 71365-364, Shiraz, Iran

Abstract: Clay-rich sediments from South Abarkouh district of clay deposit (SADC) in central Iran were analyzed for mineralogical and chemical composition, including the Rare earth element contents. Fifteen clay deposits have been located in Lower Permian (Artinskian) sediments of the area. The sediments are dominated by kaolinite, illite and quartz and minor phases include chlorite, albite, goethite, paragonite, natroalonite and gypsum. Whole rock chemistry shows that sediment samples rich in SiO_2 and Al have low Fe, Sc and Cr contents. The high Chemical Index of Alteration (CIA) values, high Chemical Index of Weathering (CIW) values, high ratio of TiO_2/Zr and low contents of the alkali and alkali earth elements of the clay-rich sediments suggest a relatively more intense weathering source area. Barium, Rb, Ca and Mg were probably flushed out by water during sedimentation. The chondrite-normalized Rare earth element patterns of the clay-rich sediments show LREE enrichments and a negative Eu anomaly. The high chondrite normalized La/Yb ratios and Gd/Yb ratios lower than 1.3, indicate that the sediments are enriched in LREEs. The mineralogical composition, REE contents, main elements discrimination diagram and elemental ratios in these sediments such as TiO_2/Al_2O_3 suggest a provenance mainly felsic rocks, with only minor contributions from basic sources. The basic sediments were most likely derived from Granitic-Riolitic rocks. The most significant geochemical finding is that despite intense weathering, which has affected most elements, the REE, Th and Sc remain immobile. The chemistry and the mineralogy of the studied samples, compared to other commercial clays, shows that they need some treatment to render them suitable for ceramics production.

Key words: Clay, South Abarkouh, mineralogy, geochemistry, REE, applications

INTRODUCTION

South Abarkouh district of clay deposit is located at the extension of the clay belt of Shahreza-Abade-Hambast (Mahjoor *et al.*, 2007a, b). This belt incorporates the richest clay deposits of Iran. The South Abarkouh district bears a high potential of clay deposits and at present, there are fifteen identified clay deposits and three active clay mines in the region. In this study, samples from three active mines were analyzed by means of geochemical and mineralogical methods in order to determining the possible Province an application of the constituting sediments of the deposits in the region.

South Abarkouh district of clay deposit is located at 60 km to the south of Abarkouh, at the southern edge of the central Iran zone and at the 10 km to the north of the metamorphic zone of Snandaje-Sirjan (Fig. 1). In fact, it is the central part of the old and eroded Bikheirkhong anticline and a part of the Hambast-Qandile mountain range (Mahjoor *et al.*, 2007b). The remaining flank of this anticline at the north and south of the Bikheirkhonge plain are in form of walls of calcareous material. These walls are composed of about 1000 m of the same slope alternative calcareous layer which belongs to the Middle to Upper Permian (Fig. 2) Permian rocks at northern and eastern walls have an extensive profile, however due to the special tectonic situation of the region and being near to the Main Zagros fault, no full cross section can be found which contains all features of the sequences. At the northern flank of Bikheirkhong plain, pass of these deposits, through the lower Permian is clearly seen (Taraz, 1972). In these sequences 5 lithologic units have been recognized and studied by Taraz (1972). The lowest unit (Unit 1) contains 400 to 450 m of 1 to 1.5 m regular dark gray calcareous beds, which overlays Lower Permian deposits with the same slope. One meter thick sandstone and calcareous sandstone layers are in the base of these layers. Samples from the lowest part of the unit contain microfossils such as *Gribrogenerina* sp., *Pseudoschwagerina* sp., *Schwagerina* sp., *Schuberetella* sp. and also macrofossils like *Juresania dorudensis*, purdella cf, Lunwallensis, these micro and macro fossils indicate the end of Early Permian (i.e. Late Artinskian).

Corresponding Author: Amir Sasan Mahjoor, Address No. 51 Shsghaiegh 3 Street, Shahid rajaie Blvd., Farhangshahr, P.O. Box 7185944736, Shiraz, Iran Tel: +989173134752 Fax: +987112350201
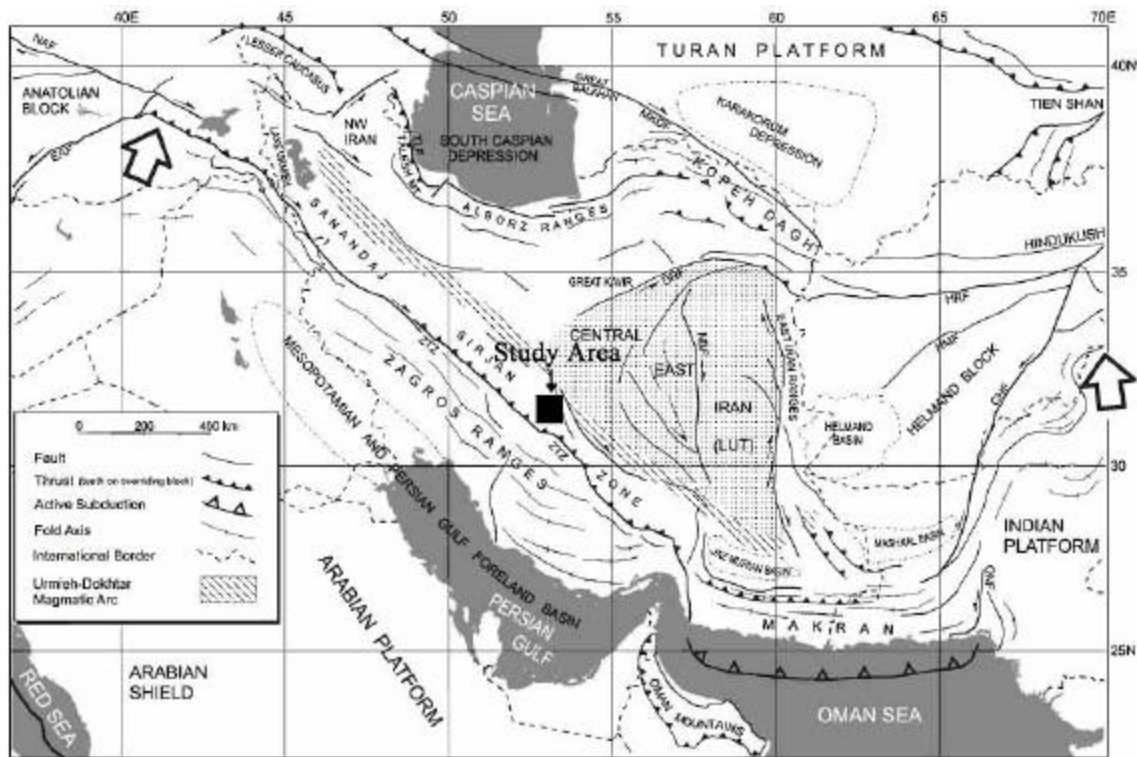
Fig. 1: Simplified structural map of Iran and adjacent regions (Compiled from: Berberian and Berberian, 1981; Alavi, 1989)

Therefore, Unit 1 shows a sequence of marine deposits that begins its procession by leaving 1 to 2 m sand stone and then several tens of meters lime in the late Artinskian. The resulted deposits, which are entirely calcareous, were then formed in the Early Mid Permian (i.e., Guadlupian) (Houshmandzadeh and Soheili, 1990). Sequences containing clay deposits of South Abarkouh district are located in the base of sandstone of Unit 1. The thickness of clay layers in the region is from 50 to 90 m. According to the Permian formation features in the region, it could be identified as Jamal formation in central Iran.

MATERIALS AND METHODS

Sampling for this study is made from three active mines at Bikheirkhong plain (Fig. 1). Since sediment sequences in all three mines are almost similar. Sampling at three mines was made from the layers underneath the sandstone's layers. This sandstone is a proper guide for following up on clay sequences in the region. The thickness of the sandstone layer varies from 60 to 80 m. In a general view, clay sequences can be divided into two entirely distinctive reddish and blackish colors. In fact, the upper 35 to 45 m of clay sequences is reddish, while

the lower 25 to 35 m is grayish black. In order to obtain better and more distinctive results, the sampling method was designed in such a way that the samples have appropriate and constant distances from one another and incorporate all the important lithological and apparent changes in the layers. Samples are taken from channels of 0.5×10×0.2 which are 12 m away from each other and parallel to the layers by counting and quartering method, in a vertical profile, from fresh surfaces. Samples are crushed by agate crusher. Clay mineral associations have been studied using X-ray diffraction. X-ray diagrams were obtained using a Phillips PW 1730 diffractometer with CuKa radiations and Ni filter. A tube voltage of 40 kV and a tube current of 25 mA were utilized. Three X-ray diagrams were performed, after air-drying, ethylene-glycol salvation and heating at 490°C during 2 h. The identification of clay minerals was made according to the position of the (001) series of basal reflections on the three X-ray diagrams (Reynolds, 1980; Moore and Reynolds, 1989) and by comparison with the Powder Diffraction File (JCPDS, 1995). Quantitative mineralogical composition was obtained using the method of Fabbri *et al.* (1986). Chemical analyses were carried out by a Philips PW 1400 XRF spectrometer,
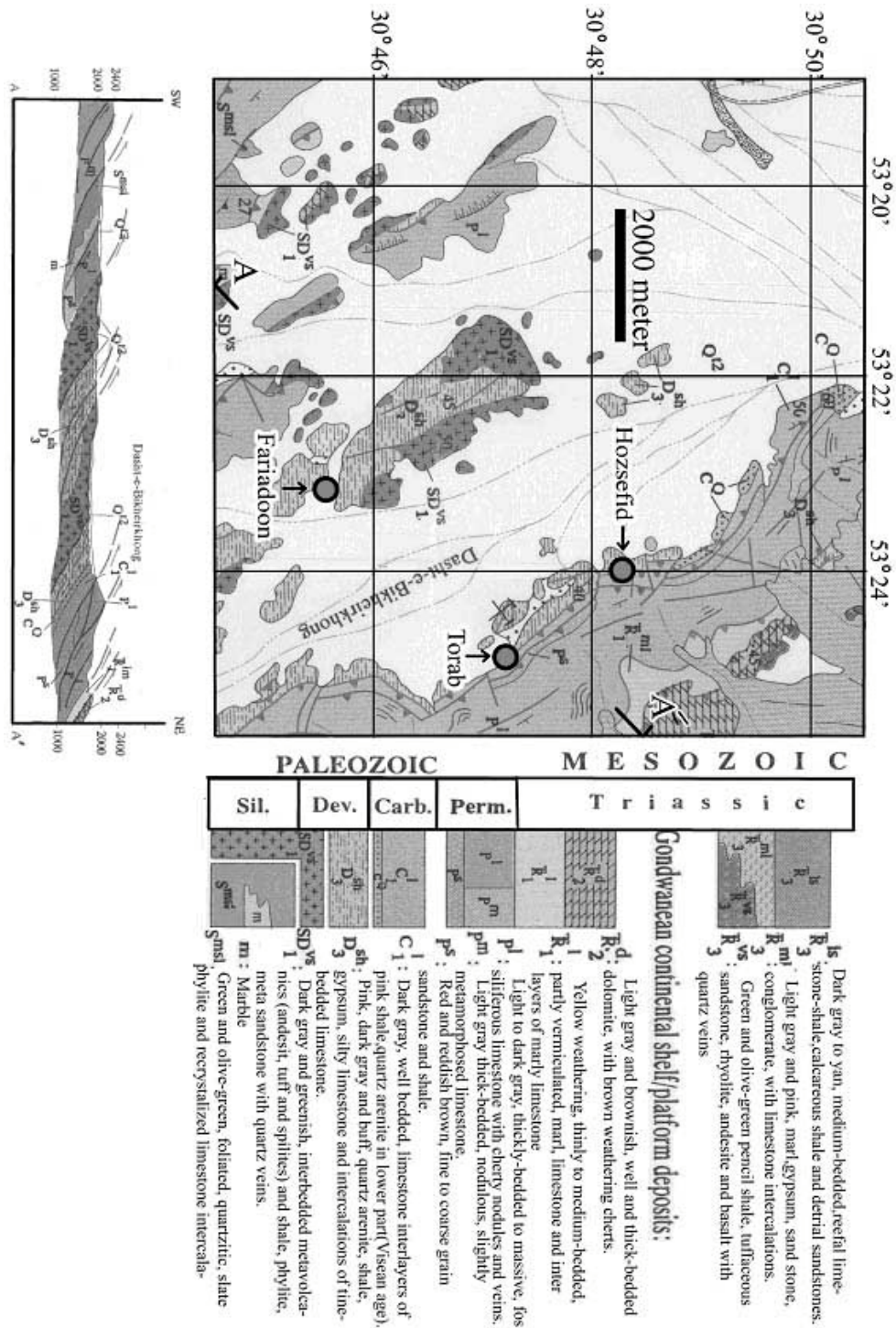
Fig. 2: Generalized geological map of study area after (Houshmandzadeh and Soheili, 1990), showing locations of the analyzed samples reported in Table 1 and 2

operating with Rh tube at 30 kV and 60 mA. Quantitative ICPMS analyzes of REE Carried out by Perkin-Elmer ELAN 6000 instrument.

RESULTS AND DISCUSSION

The XRD patterns of all whole-rock samples indicate the predominating presence of, Illite, Quartz and Kaolinite and iron mineral. Peaks were observed, indicating that goethite was incorporated in the clay minerals. Chlorite is present in trace amounts in samples. Identification of secondary minerals was difficult, because their peaks tended to be obscured by the greater peaks of the major minerals kaolinite, illite and quartz. Semi-quantitative analyses, showed differences in bulk mineral compositions between the individual sediments and also in the composition of blackish and reddish series of the sediment (Table 1).

Difference between amount of clay minerals in reddish and blackish series is obvious. For example, the kaolinite content varies from 9 wt.% in FA-1 to 61 wt.% in FA-5 in Fariadoon samples and the average amount of kaolinite differs from 20.8 wt.% in Hozsefid to 33 wt.% in Fariadoon samples. It seems that the samples much richer in quartz being poorer in kaolinite. Samples from same depths in three study locations are close in bulk mineral composition. Samples from reddish series contain high amounts of quartz and illite and minor amount of kaolinite. Samples from Blackish series contain high amounts of kaolinite and quartz and minor amount of illite. 0.5 to 3 cm thick layer intersecting veins of secondary quartz are dispersed in both reddish and blackish series layers. Dispersion and thickness of these veins in reddish series are more abundant and this is the principle reason for the abundance of quartz in reddish series in comparison with blackish series. Almost all the samples consist of small

amounts of some secondary minerals such as Gypsum, natroalonite and paragonite. These minerals are the product of interaction between leached sulfuric solutions from upper layers with some clay minerals such as illite in clay reach sediments. Reducing content of these minerals from top to bottom in study profile and the appearance of these minerals in joints and cracks support this interpretation. A sudden reduction in the content of these secondary minerals in the boundary of the reddish and blackish series of clay sediments is obvious. All sediments are, therefore, rich in kaolinite, illite and quartz, which indicate that they are derived mainly from felsic sources.

Geochemistry of the sediments: Table 2 lists the results of the major, trace elements and REE analyses for the Study area sediments compared to the average compositions of the Upper Crust (UC) and the North American Shale Composite (NASC), from Gromet *et al.*, (1984). As expected from weathered rocks, there is a large variation in the major element content for all analyzed samples. For example, the SiO_2 contents range from 48.82 to 70.35 wt.%, the TiO_2 content from 0.99 to 2.5 wt.%, the Al_2O_3 content from 14.94 to 29.2 wt.% and the Fe_2O_3 content ranges from 1.12 to 7.83 wt.%. SiO_2/Al_2O_3 ratios of samples vary from 1.8 to 4.3, which are lower than UC and NASC. The contents of MgO, CaO and MnO are all low. The Na_2O and K_2O contents range from 0.31 to 2.33 wt.% and from 0.93 to 3.01 wt.% respectively. K_2O/Na_2O ratio for the samples are obviously lower than NASC and mostly Higher than UC.

Nesbitt and Young (1982, 1996) and Nesbitt *et al.* (1996) used the ternary diagrams Al_2O_3-$(CaO+Na_2O)$-K_2O (the A-CN-K), diagram and Fe_2O_3+MgO-$(CaO+Na_2O+K_2O)$-Al_2O_3 (the A–CNK-FM), diagram to deduce weathering trends. On both the A-CN-K diagram

Table 1: Semi-quantitative (wt.%) mineralogical composition of Torab, Hozsefid and Fariadon mines, in South Abarkouh District, analyzed by X-ray diffractometry

	Sample	Sequence color	Kaolinite	Chlorite	Quartz	Illite	Albite	Gypsum	Goethite	Paragonite	Natroalonite
Torab	TR-1	Red	13	5	35	30	3	4	3	2	4
	TR-2	Red	20	7	32	32	2	3	2	0	2
	TR-3	Red	15	5	40	32	2	1	2	2	0
	TR-4	Black	50	6	19	18	2	2	1	0	2
	TR-5	Black	46	6	21	25	2	0	0	0	0
Hozsefid	HZ-1	Red	10	2	50	24	3	4	2	1	4
	HZ-2	Red	12	3	53	25	2	1	3	1	0
	HZ-3	Red	13	5	49	27	2	0	3	0	2
	HZ-4	Black	36	4	36	18	2	2	1	0	0
	HZ-5	Black	33	5	42	17	2	0	0	0	0
Fariadoon	FA-1	Red	9	6	46	17	3	3	4	10	1
	FA-2	Red	15	-	39	22	3	1	5	11	2
	FA-3	Red	31	4	47	7	2	0	4	6	0
	FA-4	Black	49	5	17	14	3	0	3	9	0
	FA-5	Black	61	9	20	9	2	0	0	0	0

Table 2: Major (wt.%) and trace (ppm) element composition of Torab, Hozsefid, and Fariadone sediments, SADC

Elements	Torab mine samples					Hozsefid mine samples					Fariadon mine samples					NASC	UC
	TR-1	TR-2	TR-3	TR-4	TR-5	HZ-1	HZ-2	HZ-3	HZ-4	HZ-5	FA-1	FA-2	FA-3	FA-4	FA-5	NASC	UC
SiO_2	53.03	55.71	53.2	57.66	57.7	61.5	66.66	69.55	70.35	68.43	49.3	48.82	52.6	52.16	56.3	64.80	66
TiO_2	1.02	1.250	1.19	2.50	1.32	1.019	1.168	1.249	1.112	1.05	1.24	0.99	1.92	1.178	1.03	0.7	0.5
Al_2O_3	23.83	23.6	24.7	25.5	25.1	18.84	17.91	14.94	16.2	14.61	27.7	26.9	27.81	23	29.2	16.9	15.2
Fe_2O_3	4.46	4.21	2.13	0.54	1.12	3.34	4.07	2.03	1.86	2.12	6.32	7.71	4.21	7.83	3.31	5.65	5
MnO	0.00	0.012	0.02	0.12	0.91	0.003	0.019	0.001	0.032	0.017	0.102	0.125	0.08	0.005	0.033	0.06	0.08
MgO	0.21	0.41	0.3	0.11	0.18	0.16	0.37	0.11	0.21	0.19	0.23	0.72	0.33	0.07	0.09	2.86	2.2
CaO	1.270	1.1	0.78	1.42	1.24	1.49	0.72	0.65	1.12	1.5	0.73	0.48	1.63	0.5	0.48	3.63	4.2
Na_2O	1.020	1.11	1.02	0.49	0.31	2.01	1.26	2.33	0.63	0.97	1.28	0.84	1.23	1.46	1.57	1.14	3.9
K_2O	2.530	2.92	3.01	1.07	0.93	1.9	1.91	2.16	1.36	1.28	2.47	1.37	2.33	1.69	1.32	3.97	3.4
P_2O_5	0.070	0.091	0.07	0.11	0.99	0.107	0.062	0.04	0.053	0.042	0.061	0.093	0.07	0.056	0.072	0.13	-
SO_3	3.500	1.5	0.33	0.7	0.02	2.563	0.296	0.83	1.66	0.06	2.72	0.237	0.63	1.436	0.21	-	-
L.O.I	7.500	6.4	11.71	8.3	8.09	8.83	6.21	7.34	7.1	5.6	10.08	10.82	8.5	10.44	11.1	-	-
CIW	91.00	93	95	93	96	93	90	83	90	85	93	94	91	92	93	-	-
CIA	85.00	84	85	91	92	84	88	78	94	82	87	91	86	95	90	-	-
K_2O/Na_2O	2.480	2.63	2.95	2.1	3	0.94	1.51	0.92	2.15	1.31	1.92	1.63	1.89	1.15	0.84	3.48	1.14
SiO_2/Al_2O_3	2.220	2.36	2.15	2.26	2.29	3.26	3.72	4.6	4.34	4.6	1.77	1.8	1.89	1.78	1.92	3.83	4.3
Cl	1620	2200	472	459	403	550	630	965	713	601	338	161	661	596	518	-	-
Ba	371	385	215	336	345	293	254	278	315	315	383	204	353	368	319	636	550
Ce	115	130	145	104	116	103	185	142	99	103	101	142	109	153	136	66.7	64
Co	8	13	7	17	20	7	9	4	18	11	8	131	5	7	18	25.7	10
Th	15	12	16	12	14	11	12	11.5	13	12	11	13	14	12	11	12.3	10.7
U	3	3	3	4	3	3	5	7	4	3	4	2	3	7	5	2.66	2.8
Cr	106	126	86	93	90	95	104	71	85	101	71	100	87	91	105	125	34
Mo	1	1	1	1	1	1	1	1	1	1	1	1	1	1	1	-	-
Cu	10	105	12	5	35	25	20	14	40	15	1	17	2	5	21	-	25
Nb	23	19	27	23	21	18	28	27	19	29	33	20	31	26	21	13	25
Ni	43	39	19	22	27	21	34	18	24	30	14	283	17	34	119	58	20
Pb	39	17	28	23	25	41	37	43	39	28	30	24	30	24	21	-	15.0
Rb	116	75	91	62	80	89	102	124	95	108	121	73	97	88	81	125	110.2
Sr	118	66	30	130	107	87	45	111	133	110	86	79	103	82	137	142	350
V	132	156	113	125	130	113	135	99	109	124	100	133	119	121	126	130	60
W	6	18	29	15	17	4	3	3	12	23	1	70	10	5	1	2.10	-
Y	30	21	30	26	23	24	26	30	33	29	26	33	29	28	24	35	22
Zr	261	243	297	288	295	258	286	298	302	276	313	259	297	302	289	200	190
Zn	63	77	90	61	40	63	102	47	69	52	50	519	100	63	254	-	71

Table 2: Continued

Elements	Torab mine samples					Hozsefid mine samples					Fariadon mine samples					NASC	UC
	TR-1	TR-2	TR-3	TR-4	TR-5	HZ-1	HZ-2	HZ-3	HZ-4	HZ-5	FA-1	FA-2	FA-3	FA-4	FA-5		
Sc	11.5	9.38	12.7	13.0	10.4	10.5	11.9	12.70	13.80	12.0	13.50	14.8	11.2	13.30	13.5	14.9	11
Th/U	5	4.3	5.3	4.2	4.6	7	3.4	3.3	5.25	6.3	5	6.5	5.3	2.6	3	4.6	3.8
TiO$_2$/ZR×100	1.6	1.6	1.3	4.1	3.3	1.6	1.1	2.7	1.6	2.0	2.5	0.2	1.9	1.9	0.4	-	0.7
La	37.1	37.3	36	45	30.3	36.88	41.3	43.1	44.4	38.8	34.9	38.6	39.1	32.25	33.31	31.1	30
Ce	67.0	77.1	73.2	69.2	72.3	65	42.2	62	70.9	70.3	79.1	61.1	72.6	64.3	69.3	64	67.03
Pr	7.51	8.16	8.30	6.04	8.33	7.06	8.23	8.08	7.9	8.68	6.58	7.44	8.47	6.58	7.3	-	7.1
Nd	21.32	26.6	25.2	24.0	23.5	24.54	26.7	23.2	32.9	34.3	28.9	26.15	22.71	29.76	31.4	30.4	26
Sm	5.33	6.04	6.24	7.06	7.15	5.21	7.94	6.03	6.45	8.24	5.36	6.3	5.41	4.61	5.55	5.98	4.5
Eu	1.68	1.82	1.91	2.12	1.02	1.71	1.62	1.79	1.19	0.99	1.71	1.06	1.65	0.98	1.02	1.25	0.88
Gd	3.32	3.51	3.82	4.52	5.71	3.18	5.52	4.57	5.34	5.81	4.62	6.2	5.64	3.74	6.04	5.5	3.8
Tb	0.92	1.19	0.83	1.03	0.77	1.14	0.85	0.96	0.88	0.62	0.69	0.73	0.71	0.83	0.81	0.85	0.64
Dy	4.8	5.32	4.66	5.01	4.98	3.69	4.09	3.77	4.21	4.36	5.05	5.92	4.51	4.13	4.56	5.54	3.5
Ho	0.84	0.92	0.93	085	0.81	0.92	0.98	0.93	0.91	1.02	1.03	1.17	1.06	1.11	1.12	-	0.8
Er	3.63	3.61	3.13	3.82	3.93	3.41	3.59	3.43	4.06	3.66	4.08	3.35	3.95	3.82	3.68	3.27	2.3
Tm	0.32	0.31	0.32	0.48	0.38	0.28	0.31	0.38	0.43	0.42	0.46	0.41	0.46	0.33	0.33	-	0.33
Yb	2.81	3.09	2.92	3.13	3.14	3.61	2.89	3.64	3.9	2.98	4.09	3.55	3.1	3.02	3.87	3.11	2.2
Lu	0.43	0.43	0.51	0.56	0.54	0.4	0.54	0.5	0.41	0.45	0.45	0.5	0.47	0.45	0.45	0.45	0.32
(Gd/Yb)c	0.98	0.94	1.08	1.19	1.50	0.73	1.38	1.04	1.13	1.61	0.93	1.44	1.31	1.02	1.29	1.46	1.43
(Eu/Eu)*	1.18	0.9	1.14	0.8	0.79	1.34	0.97	0.8	0.94	0.8	0.87	0.86	0.79	1.05	0.82	0.66	0.65
(La/Yb)c	9.9	8.7	9.8	10.3	7.9	7.3	10.3	9.5	8.2	10.1	7.1	10.8	9.9	9.7	7.2	7.2	9.8
La/Sc	3.2	4	2.8	3.5	2.9	3.5	3.5	3.4	3.2	3.2	2.6	2.6	3.5	2.4	2.5	2.1	2.7
La/Th	2.5	3.1	2.3	3.8	2.2	3.4	3.4	3.7	3.4	3.2	3.2	3.0	2.8	2.7	3.0	2.5	2.8
Th/Sc	1.3	1.3	1.3	0.9	1.3	1.0	1.0	0.9	0.9	1.0	0.8	0.9	1.3	0.9	0.8	0.8	1.0

Major elements as wt.% and trace elements in ppm. Total Fe as Fe$_2$O$_3$, CIA = [Al$_2$O$_3$/(Al$_2$O$_3$+CaO+Na$_2$O+K$_2$O)]×00 and CIW = [Al$_2$O$_3$/(Al$_2$O$_3$+CaO+Na$_2$O)]×100 in molecular proportions. CaO in both CIA and CIW is CaO in silicate fraction only and was corrected following the McLennan (1993) method. UC = Upper Crust after Taylor and McLennan (1985) and NASC = Average North American Shale after Gromet *et al.* (1984). Eu/Eu* = Eucn/ [(Smcn)(Gdcn)]
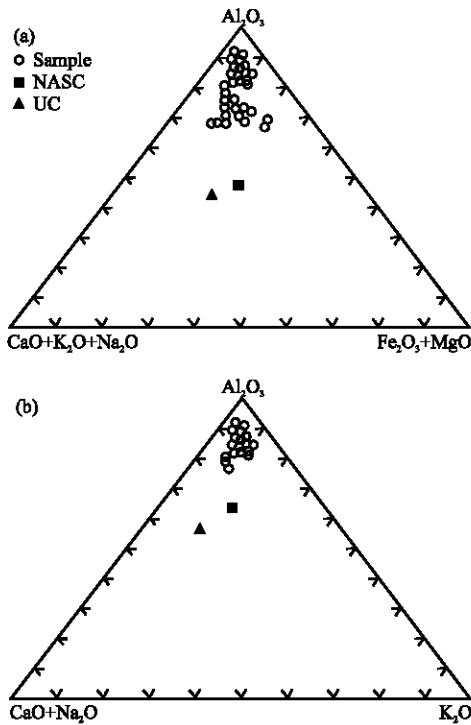
Fig. 3: (a) Triangular Al$_2$O$_3$-(CaO+Na$_2$O+K$_2$O)-Fe$_2$O$_3$+
MgO plot of sediment samples (after Nesbitt and
Young, 1980, 1982, 1996; Nesbitt *et al.*, 1996). (b)
Al$_2$O$_3$-(CaO+Na$_2$O)-KO$_2$ plot of sediment samples
(after Nesbitt and Young, 1980, 1982, 1996;
Nesbitt *et al.*, 1996) and Upper Crust (UC) given by
Taylor and McLennan (1985) and North American
Shale Composite (NASC) given by Gromet *et al.*
(1984).

(Fig. 3b) and the A-CNK-FM diagram (Fig. 3a), all the
sediments display an intense weathering history. The
sediments plot in a region clearly suggesting different
relative contents in Al$_2$O$_3$, CaO, Na$_2$O and K$_2$O from those
NASC and UC and plot closer to high Al$_2$O$_3$ contents,
which is suggestive of a relatively high intensity of
weathering. Weathering has proceeded to a stage at
which significant amounts of the alkali and alkali earth
elements were removed from the sediments.

**Two chemical weathering indices have been
proposed:** Chemical Index of Alteration (CIA) (Nesbitt and
Young, 1982) and Chemical Index of Weathering (CIW)
(Harnois, 1988). Nesbitt and Young (1982) reported a CIA
value of nearly 100 for Kaolinite and chlorite and 70 to 75
for average shale's, whereas Taylor and McLennan (1985)
reported a CIA value of 85 to 100 for residual clays.
Condie (1993) reported that most post-Archean shale's
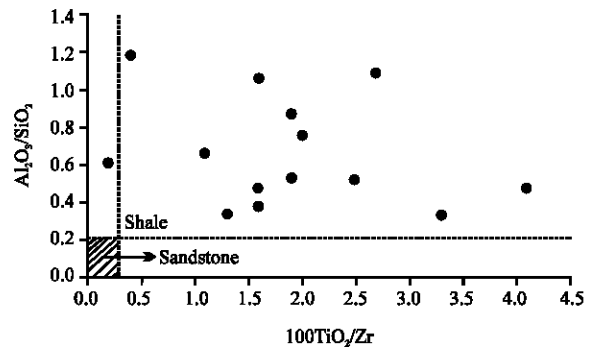
Fig. 4: Al$_2$O$_3$/SiO$_2$ vs. 100TiO$_2$/Zr diagram for SADC
samples (after Garcia *et al.* (1994)
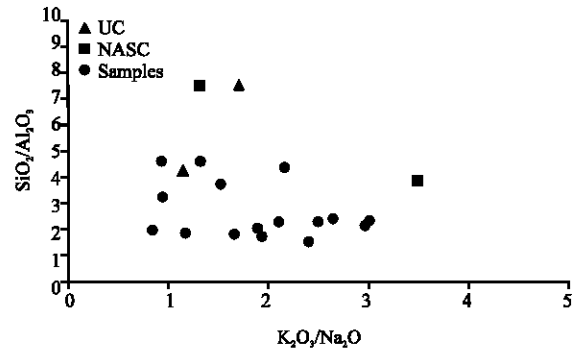
Fig. 5: SiO$_2$/Al$_2$O$_3$ vs. K$_2$O/Na$_2$O diagram for SADC

show moderate losses of Ca, Na and Sr from source
weathering, with CIW values of 80 to 95 and Sr contents
of 75 to 200 ppm. In contrast, most Archean shales, show
greater losses of all three elements, with CIW of 90 to 98
and Sr contents <100 ppm. The CIA of the sediments
varies between 82 to 95, which is high compared to UC
and NASC, but close to that of kaolinite (Table 2). The
CIW, which does not include K$_2$O, ranges between
90 to 96, with Sr contents ranging from 62 to 124 ppm.

The CIA and CIW are both higher than those of
average shales, suggesting relatively intense source area
weathering. The high CIA and CIW values in the
sediments probably reflect the presence of clay minerals
and absence of detrital feldspars. High ratio of TiO$_2$/Zr
(0.011-0.022) indicates the maturity of South Abarkouh
samples (Ugidos *et al.*, 2003) (Fig. 4). Therefore, the South
Abarkouh sediments are more mature than post-Archaean
shales such as NASC (Condie *et al.*, 1995) (Fig. 5).

TRACE ELEMENT GEOCHEMISTRY

The behavior of trace elements during sedimentary
processes is complex due to factors including weathering,

physical sorting, adsorption, provenance, diagenesis and metamorphism (e.g., Nesbitt *et al.*, 1980; Taylor and McLennan, 1985; Wronkiewicz and Condie, 1987; Condie *et al.*, 1995; Manceau *et al.*, 2000; Roddaz *et al.*, 2006). The trace element data show moderate variations compared to NASC and UC (Table 2). All sediments have similar contents in trace elements and are almost enriched in Y, Zr, Nb, Th and U. These elements are associated with heavy minerals, such as zircon, which is resistant to weathering. They are preferentially partitioned into melts during crystallization and anatexis (Feng and Kerrich, 1990; Böning *et al.*, 2004) and as a result, these elements are enriched in felsic rather than mafic rocks. Thorium and U behave differently during weathering, as U, unlike Th, is chemically mobile as U6+ and there is a tendency of the Th/U ratio to be elevated above upper crustal values of 3.5 to 4.0 (McLennan *et al.*, 1993). The sediments show Sc, V, Zn, Ni and Cr, contents similar to, or even above, abundances for NASC. However, they are depleted in Co, Cu, Rb, as well as in Sr and Ba contents. Generally these elements are associated with clay minerals and their low values could be attributed to the low values in parent rocks and the high quartz content in the sediments (Table 1). This is in agreement with studies by Nesbitt *et al.* (1980), Wronkiewicz and Condie (1987) and Böning *et al.* (2004), in which these authors conclude that small cations, such as Na, Ca and Sr, are selectively leached and weathered from weathering profiles, whereas cations with relatively large ion radii, such as K, Cs, Rb and Ba, may be fixed by preferential exchange and adsorption on clays. Therefore, in general, weathering conditions were more intense in the source area before sedimentation. Strontium and barium mostly reside in plagioclase and K-feldspar, respectively (Picouet *et al.*, 2002). The fractionation of these two elements can result from the selective weathering of these feldspars. Weathering of plagioclase will decrease the Sr content, because plagioclase is more easily weathered than K-feldspar and Sr is more mobile than Ba. A depletion of Ba could be due to recrystallization of clays and progressive destruction of feldspars. Potassium, Rb and Cs are mainly hosted in micas and K-feldspar (Picouet *et al.*, 2002); thus, alteration of these minerals will dominate the fractionation of these elements. Rubidium has a trend comparable to that of Nb and V and is less mobile than K, whose behavior it otherwise follows. Rubidium with respect to K is preferentially retained in weathered illite (Garrels and Christ, 1965). Nb and V are less mobilized, in agreement with what is known about their behavior during weathering (Middleburg *et al.*, 1988).

RARE-EARTH ELEMENT VARIATIONS

All analyzed sediment samples have similar concentrations of the REEs. Chondrite-normalized patterns are typical for shale in general, with an enrichment of the LREEs.

Samples have pronounced negative Eu anomalies. The Eu anomaly parallels the depletion in Na_2O and CaO, suggesting that it developed at least partially in response to plagioclase weathering, where most of the Eu is hosted. The Eu anomaly in sedimentary rocks is usually interpreted as being inherited from igneous source rocks (McLennan and Taylor, 1991; McLennan *et al.*, 1980;
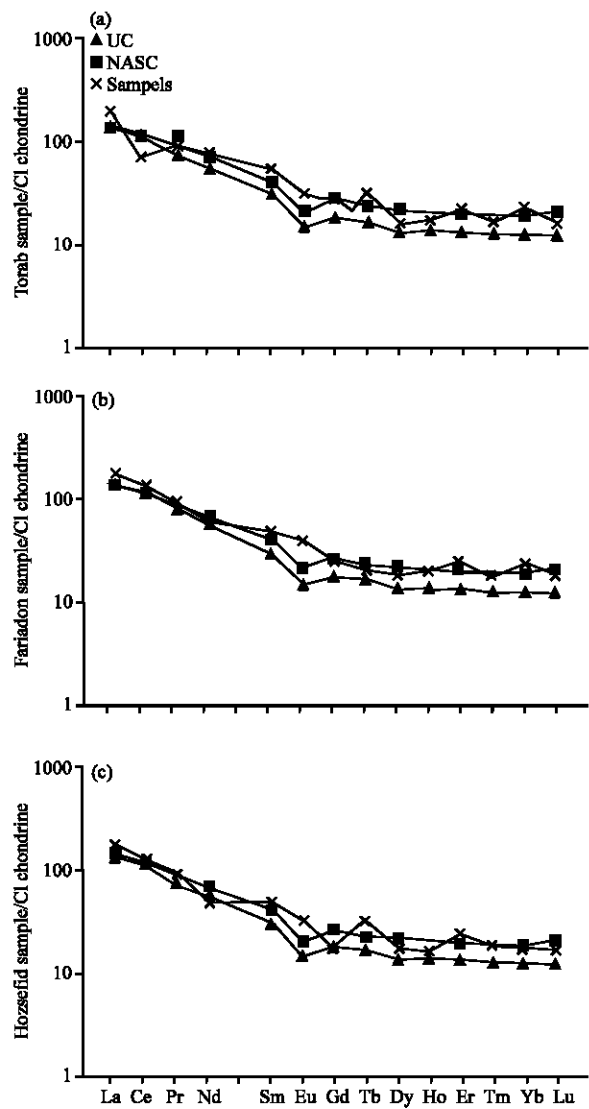

Fig. 6: Rare earth element plots of (a) Torab, (b) Fariadon and (c) Hozesfid samples normalized to Cl chondrites after Taylor and McLennan (1985)

Awwiller, 1994; Compton *et al.*, 2003). Figure 6 shows that despite the difference in the absolute abundances, the samples show REE patterns that are similar to NASC, but differ in the HREE content compared to the UC. The chondrite-normalized La/Yb ratio ranges from 6.2 to 10.2, with most sediment having slightly higher values than UC. The relative depletion in the HREEs compared to LREEs may be due to a lower concentration of heavy minerals, for example zircon. The low abundances of Zr in the sediments (Table 2) support this interpretation.

Provenance: The REEs and high field strength elements (HFSE, including Y, Zr, Ti, Nb and Ta), Th, Sc, Hf and Co are the most suitable ones for provenance determination, because of their relatively low mobility during weathering, transport, diagenesis and metamorphism. Ratios of both incompatible and compatible elements are useful for differentiating between felsic and mafic source components. In addition, the REE patterns have been also used to infer sources of sedimentary rocks, since basic rocks contain low LREE/HREE ratios and no Eu anomalies, whereas more silicic rocks usually contain higher LREE/HREE ratios and negative Eu anomalies (Cullers and Graf, 1983). Therefore, the REE patterns of the source rocks may be preserved in sedimentary rocks (Taylor and McLennan, 1985; Wronkiewicz and Condie, 1987, 1989; Condie *et al.*, 1995; Compton *et al.*, 2003). Mineralogical maturity of the sediments indicated by the proportion of compositionally mature alumina-rich minerals such as kaolinite is consistent with having a felsic or reworked sedimentary source (Roddaz *et al.*, 2006; Cullers *et al.*, 1975, 1987). The CIA, which varies from 78 to 95 and the CIW values (90 to 96) point towards a more felsic source and may indicate sediment recycling processes (Nesbitt *et al.*, 1980). Ekosse (2001) suggested the ratio of TiO_2/Al_2O_3 as a province indicator. From Fig. 7, the TiO_2/Al_2O_3 plot indicates provenance of materials from predominantly granite-rhyolite. In discrimination diagram for sedimentary provenance (Roser and Korsch, 1988). The South Abarkouh clay samples plot in felsic igneous and quartzose sedimentary province fields (Fig. 8).

The sediments have fractionated REE patterns, with slightly high ratio of $(La/Yb)_{cn}$ and a negative Eu anomaly. The LREEs are enriched and HREE pattern are almost flat, with low ratio of $(Gd/Yb)_{cn}$. These characteristics indicate that the original source area was felsic and the negative Eu anomaly is regarded as evidence for a differentiated source, similar to granite (McLennan, 1989; McLennan *et al.*, 1993; Taylor and McLennan, 1985, 1995). The relative enrichments of incompatible elements (e.g., LREE, Th) over compatible elements (e.g., Sc, Co) in
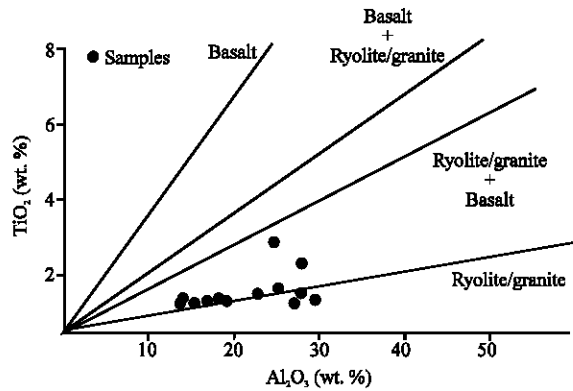
Fig. 7: Position of South Abarkouh district of clay deposits samples on TiO_2/Al_2O_3 binary diagram suggested by Ekosse (2001)
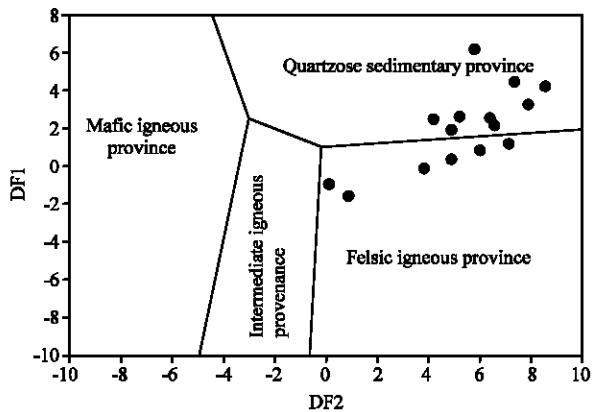
Fig. 8: Discrimination diagram for Sedimentary provenance of South Abarkouh clay sediments (Roser and Korsch, 1988). DF1 = [56.50 TiO_2-10.879 Fe_2O_3(total)+30.875 MgO-5.404Na_2O+ 11.112K_2O]/Al_2O_3-3.89. DF2 = [30.638TiO_2-12.541Fe_2O_3(total)+7.32MgO+12.031Na_2O+ 35.402K_2O]/Al_2O_3-6.382

the sediments, indicate relatively felsic average provenance compositions and a relatively severe weathering regime (McLennan *et al.*, 1993; Krogstad *et al.*, 2004). The slight differences among the REE patterns probably do not reflect changes in source area composition, but are likely due to variations in mineral sorting and weathering.

The immobile elements La and Th are more abundant in felsic than in basic rocks, whereas Sc and Co are more concentrated in basic rocks than in felsic rocks (Taylor and McLennan, 1985; Wronkiewicz and Condie, 1987; Condie *et al.*, 1995). It has been shown that ratios, such as La/Sc, Th/Sc, Co/Th, Cr/Th and Eu/Eu*, in
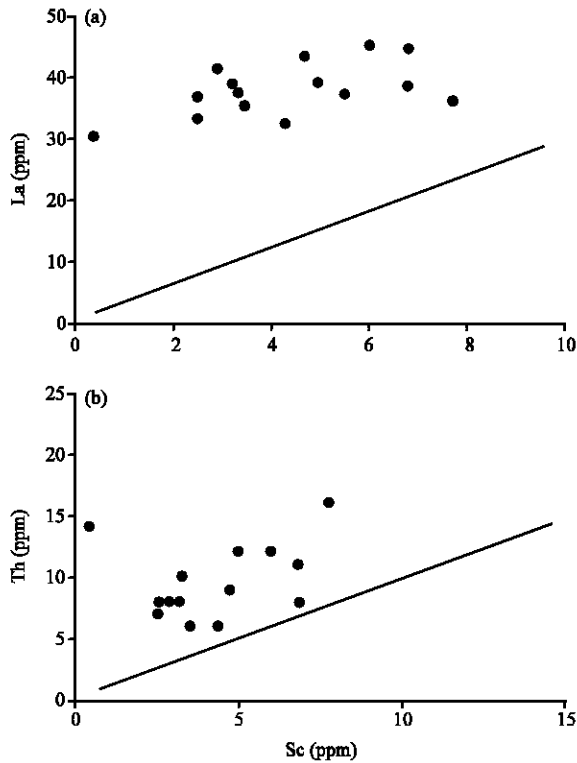
Fig. 9: (a) Th versus Sc for sediment samples. (b) La versus Sc for sediment samples. Th/Sc = 1 and La/Sc = 3 ratio is that of the upper continental crust (UC)
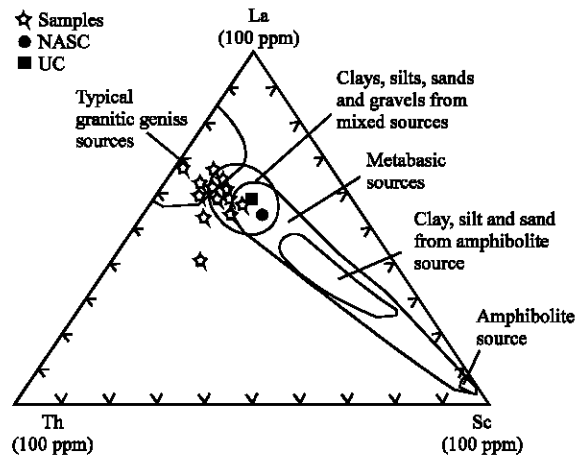

Fig. 10: Ternary plot of La-Th-Sc for the sediment samples after Cullers (1994a) compared with Upper Crust (data from Taylor and McLennan, 1985) and North American Shale Composite (data from Gromet *et al.*, 1984)

siliciclastic sediments, can place constraints on the average provenance composition (Cox *et al.*, 1995; Cullers, 1994b, 1995; Cullers *et al.*, 1988; Wronkiewicz and Condie, 1987, 1989, 1990; Condie *et al.*, 1995). Thus, the concentration of these elements and the corresponding elemental ratios in sediments may be useful for provenance determination. The geochemical differences between elements such as Th and La (indicative of a felsic source) and Sc and Cr (indicative of a mafic source) have been exploited to distinguish between felsic and mafic provenance by various authors (McLennan, 1989; McLennan and Taylor, 1991; McLennan *et al.*, 1980; Wronkiewicz and Condie, 1990; Condie *et al.*, 1995; Krogstad *et al.*, 2004). The Th versus Sc and La versus Sc plots (Fig. 9a, b) shows that the sediment data scatter above the Th/Sc = 1 and La/Sc = 3 lines with most samples that have Sc contents below 10 ppm indicating a more felsic component. The Th/Sc and La/Sc values are higher than that of UC. The ratios of Th/Sc range from 1.6 to 2.8 and La/Sc from 2 to 5, suggesting a felsic source of sediments (Weber *et al.*, 1998).

In a La-Th-Sc diagram (Fig. 10), which is used to discriminate felsic and basic provenance of finegrained sediments (Cullers, 1994a, b), the sediment data fall in a region that indicates a predominantly felsic source, but does not exclude an intermediate source or possible mixing between felsic and basic source rocks. The sediment data show a cluster along the La-Th edge, at a position closer to La than to Th indicating that La, Th and Sc have been removed in weathered profiles. The sediments have low contents of Sc, Fe, REE, Th, Hf and Cr (and Co), high La/Sc, Th/Sc, La/Cr, Th/Cr and Ba/Sc ratios, which indicates that they were derived mainly from felsic rocks (Cullers *et al.*, 1987, 1988; Cullers, 1988; Roddaz *et al.*, 2006) rather than from basic rocks. The sediments with a basic component were most likely derived from metasedimentary rocks, such as muscovite-biotite schists. Thus, on the basis of chemical composition, the sediments are derived locally, mainly from highly acidic rocks, with minor contributions from basic rocks.

Application: The chemical data were plotted in a ternary diagram (silica-alumina-other oxides), as used by Fabbri and Fiori (1985) to classify raw materials and industrial ceramic bodies (Fig. 11). This diagram shows ceramic compositional fields and reflects the overall chemical composition of SADC raw materials. In this diagram, some samples plot into the white bodies' field, but most of the samples do not. Taking into account the ideal composition for an optimum white body product according to the mentioned authors (SiO_2 = 72 wt.%,
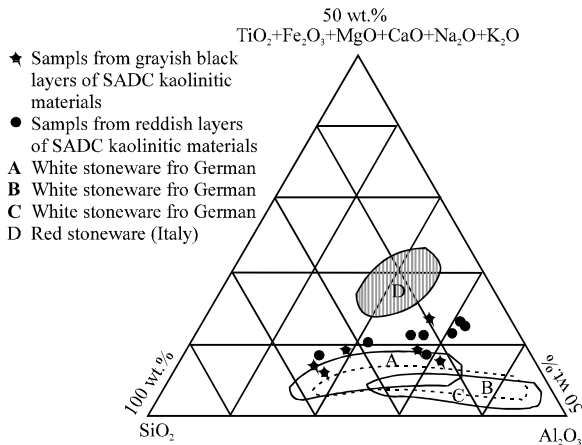
Fig. 11: Triangular diagram of SADC clays: $SiO_2 = Al_2O_3$ = total oxides are plotted, (data from Fabbri and Fiori, 1985)
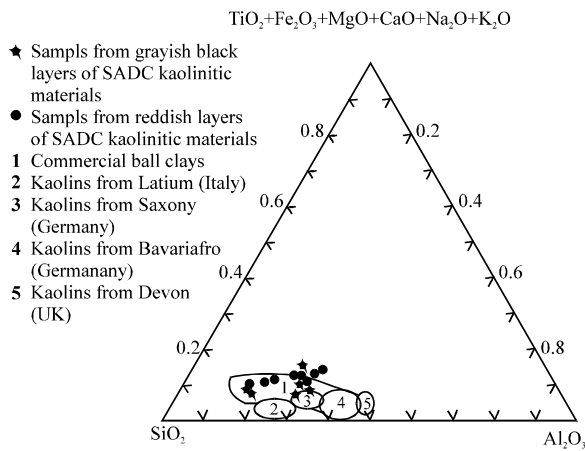

Fig. 12: Ternary diagram SiO_2-Al_2O_3-other oxides of the kaoliniteic materials from the SADC district and comparison with the Chemical composition of commercial kaolins (Ligas *et al.*, 1997) and ball clays (after Fabbri and Fiori, 1985)

Al_2O_3 and total oxides = 8 wt.%), samples outside the white bodies field need processing. From their chemical composition, they could be considered as raw material for use in structural ceramic products (Konta, 1995). From chemical and mineralogical analysis, the studied clay samples are ball clays (Fig. 12 Bergaya *et al.*, 2006).

The mineralogical and chemical composition of the SADC kaolins shows both favorable and adverse aspects for ceramic applications. These materials already use in ceramic industry.

The favorable characteristics are:

- A simple mineralogical association, mainly represented by kaolinite and illite plus silica phases
- The prevalence of kaolinite and illite to other minerals
- The low iron amount, particularly if referred to a clay material, which allows these kaolins to be potentially used in white body production (Murry, 2007)

Nevertheless, the most relevant limitation, which could cause many problems in the ceramic manufacturing, is abundance of silica phases, prevailing on clay minerals, making these materials less plastic to be used as ceramic raw material. Pb in SADC kaolin makes it difficult to be used in both the pharmaceutical and paper industries. For the SADC kaolin to be used in the rubber and plastic industries, metals such as Mn, Fe and Cu should not exceed 5 ppm and soluble salts present is removed. The beneficiation processes may be expensive for any profit to be realized. Further beneficiation tests are needed for it to be considered for other industrial applications such as plaster, crayons, pesticides and insecticides.

CONCLUSION

We analyzed 15 samples from three locations in South Abarkouh district of clay deposite (SADC), in order to determine their mineralogical and chemical compositions, REE characteristics, provenance and possible applications. XRD analyses show that the sediments are dominated by kaolinite, illite and quartz, with minor, chlorite, albite, gypsum, paragonite, natroalonite and goethite. From the weathering diagrams (Fig. 4, 5), it is possible to infer that the samples underwent a relatively high degree of weathering. Weathering has proceeded to a stage where a major part of the alkali and alkali earth elements were removed. The low CaO contents in sediments indicate their maturity relative to most typical post-Archean shales, such as NASC. The sediments are depleted in Ca, Na and Sr compared to Archean shale compositions (Condie, 1993; Condie *et al.*, 1995). CIW values of around 93 and variations in CIA values from 82 to 95, indicate that the sediments contain residual clays rich in kaolinite (Taylor and McLennan, 1985). The low contents of Sc, Fe, REE, Th, Hf and Cr (and Co), and high La/Sc, Th/Sc, La/Cr, Th/Cr and Ba/Sc ratios in the sediments, all indicate that the sediments were derived from granitic rocks. This also agrees with the general shape of the chondrite-normalized REE patterns (including a negative Eu anomaly). The slight increase in the LREE is probably a source area effect. Mineralogical and geochemical data

here reported that the provenance of the sediments was dominated by felsic sources. The basic component in the sediments was most likely derived from metasedimentary rocks, such as muscovite-biotite schists, while the felsic sediments are derivatives of granitoid rocks. We find that, despite intense weathering, which affected the contents of most elements, the REE, Th and Sc remained immobile; this observation can be considered as one of the most important geochemical results of the present study.

Even though all these materials are currently exploited in the production of various ceramic products, most of them are not comparable to commercially marketed European counterparts Nevertheless, the studied samples show interesting features for application in the ceramic sector if well treated, especially considering the high iron oxide content. However, due to the generally high quartz contents they may possess a refractory behavior. These clays have chemical and mineralogical compositions that indicate their useful for brick, ceramic and earthenware production. Further systematic applied testing of the clays has yet to be carried out to determine their physical, mechanical and technological properties

REFERENCES

Alavi, M., 1989. Tectonic map of the Middle East. Geological Survey of Iran. Tehran.

Awwiller, D.N., 1994. Geochronology and mass transfer in gulf coast mudrocks (South-Central Texas, USA): Rb-Sr, Sm-Nd and REE systematics. Chem. Geol., 116: 61-84.

Berberian, F. and M. Berberian, 1981. Zagros, Hindu Kush, Himalaya, Geodynamic Evolution: Geodynamics Series 3. 1st Edn., Am. Geophysical Union, Washington, D.C., pp: 5-32.

Bergaya, F., B. Theng and G. Lagary, 2006. Handbook of Clay Science. 1st Edn., Elsevier, Amesterdam, ISBN-13: 978-0080441832.

Böning, P., H. Brumsack, M. Böttcher, B. Schnetger and C. Kriete *et al.*, 2004. Geochemistry of peruvian near-surface sediments. Geochimica Cosmochimica Acta, 68: 4429-4451.

Compton, J.S., R.A. White and M. Smith, 2003. Rare earth element behavior in soils and salt pan sediments of a semi-arid granitic terrain in the Western Cape, South Africa. Chemical Geol., 20: 239-255.

Condie, K.C., 1993. Chemical composition and evolution of the upper continental crust: Contrasting results from surface samples and shales. Chem. Geol., 104: 1-37.

Condie, K.C., J. Dengate and R.L. Cullers, 1995. Behavior of rare earth elements in a paleoweathering profile on granodiorite in the front range, Colorado, USA. Geochimica Cosmochimica Acta, 5: 279-294.

Cox, R., D.R. Lowe and R.L. Cullers, 1995. The influence of sediment recycling and basement composition on evolution of mudrock chemistry in the south-western United States. Geochim. Cosmochim. Acta, 59: 2919-2940.

Cullers, R.L., S. Chaudhuri, B. Arnold, M. Lee and C.W. Wolf, 1975. Rare earth distributions in clay minerals and in clay-sized fraction of the lower permian havensville and eskridge shales of kansas and oklahoma. Geochim. Cosmochim. Acta, 39: 1691-1703.

Cullers, R.L. and J. Graf, 1983. Rare Earth Elements in Igneous Rocks of the Continental Crust: Intermediate and Silicic Rocks, Ore Petrogenesis. In: Rare-Earth Geochemistry, Henderson, P. (Ed.). Elsevier, Amsterdam, pp: 275-312.

Cullers, R.L., T. Barrett, R. Carlson and B. Robinson, 1987. Rare-earth element and mineralogic changes in holocene soil and stream sediment: A case study in the wet mountains region, Colorado, USA. Chem. Geol., 63: 275-297.

Cullers, R.L., 1988. Mineralogical and chemical changes of soil and stream sediment formed by intense weathering of the Danburg granite, Georgia, USA. Lithos, 21: 301-314.

Cullers, R.L., A. Basu and L. Suttner, 1988. Geochemical signature of provenance in sand-size material in soils and stream sediments near the Tobacco Root batholith, Montana, USA. Chem. Geol., 70: 335-348.

Cullers, R.L., 1994a. The chemical signature of source rocks in size fractions of holocene stream sediment derived from metamorphic rocks in the wet mountains region, Colorado, USA. Chem. Geol., 113: 327-343.

Cullers, R.L., 1994b. The controls on the major-and trace-element variation of shales, siltstones and sandstones of Pennsylvanian-Permian age from uplifted continental blocks in Colorado to platform sediments in Kansas, USA. Geochim. Cosmochim. Acta, 58: 4955-4972.

Cullers, R.L., 1995. The controls on the major- and trace-element evolution of shales, siltstones and sandstones of ordovician to tertiary age in wet mountains region, Colorado, USA. Chem. Geol., 123: 107-131.

Ekosse, G., 2001. Provenance of the kgwakgwa kaolin deposit in southeastern botsowana and its possible utilization. Applied Clay Sci., 20: 137-152.

Fabbri, B. and C. Fiori, 1985. Clays and complementary raw materials for stoneware tiles. Mineralogica Petrographica Acta, 29A: 535-545.

Fabbri, B., C. Fiori, A. Krajewski, R. Valmori and A. Tenaglia, 1986. Comparison between traditional mineralogical and computerized rational analysis of ceramic raw materials. J. Phys. Colloque C1. Suppl., 47: 1-57.

Feng, R. and R. Kerrich, 1990. Geochemistry of finegrained clastic sediments in the Archean Abitibi greenstones belt, Canada: Implications for provenance and tectonic setting. Geochim. Cosmochim. Acta, 54: 1061-1081.

Garrels, R.M. and C.L. Christ, 1965. Solutions, Minerals and Equilibria. 1st Edn., Freeman and Cooper, San Francisco, California, pp: 450-450.

Gromet, L.P., R.F. Dymek, L.A. Haskin and R.L. Korotev, 1984. The North American Shale Composite: Its compilation, major and trace element characteristics. Geochim. Cosmochim. Acta, 48: 2469-2482.

Harnois, L., 1988. The CIW index: A new chemical index of weathering. Sediment. Geol., 55: 319-322.

Houshmandzadeh, A. ans M. Soheili, 1990. Explanatory text of the eqlid quadrangle map 1:25000. Geological Survey of Iran, pp: 157.

JCPDS, 1995. Powder diffraction file, inorganic phases. Int. Centre for Diffraction Data, Newtown Square, PA, USA.

Konta, J., 1995. Clay and man: Clay raw materials in the service of man. Applied Clay Sci., 10: 271-273.

Krogstad, E., C.M. Fedo and K.A. Eriksson, 2004. Provenance ages and alteration histories of shales from the middle archean buhwa greenstone belt, Zimbabwe: Nd and Pb isotopic evidence. Geochimica Cosmochimica Acta, 68: 319-332.

Ligas, P., I. Uras, M. Dondi and M. Marsigli, 1997. Kaolinitic materials from romana (North-West Sardinia), Italy and their ceramic properties. Applied Clay Sci., 12: 145-163.

Mahjoor, A.S., M. Karimi and A. Rastegarlari, 2007a. Study of mineralogy, geochemistry and possible genesis of torab clay deposit (south Abarkouh). MS Thesis. Islamic Azad University (Shiraz Branch), Iran, pp: 136.

Mahjoor, A.S., M. Karimi, S. Liaghat and A. Rastegarlari, 2007b. The study of geology, geochemistry, mineralogy and evaluation of the industrial applications of Torab clay deposit in South Abarkouh, a none reported case of Global clay genesis evidence in Permoterias. Isfahan Univ. J. Sci., 29: 23-42.

Manceau, A., M.L. Schlegel, M. Musso, V.A. Sol and L. Gautheire *et al.*, 2000. Crystal chemistry of trace elements in natural and synthetic goethite. Geochem. Cosmochem. Acta, 64: 3643-3661.

McLennan, S.M., W.B. Nance and S.R. Taylor, 1980. Rare earth element-thorium correlations in sedimentary rocks and the composition of the continental crust. Geochim. Cosmochim. Acta, 44: 1833-1839.

McLennan, S.M., 1989. Rare earth elements in sedimentary rocks: Influence of provenance and sedimentary processes. Geochemistry and mineralogy of the rare earth elements. Rev. Mineral. Geochem., 21: 169-200.

McLennan, S.M. and S.R. Taylor, 1991. Sedimentary rocks and crustal evolution: Tectonic setting and secular trends. J. Geol., 99: 1-21.

McLennan, S.M., 1993. Weathering and global denudation. J. Geol., 101: 295-303.

McLennan, S.M., S. Hemming, D.K. McDaniel and G.N. Hanson, 1993. Geochemical Approaches to Sedimentation, Provenance and Tectonics. In: Processes Controlling the Composition of Clastic Sediments, Johnson, M.J. and A. Basu (Eds.). Geological Society of American Special Paper, USA., pp: 21-40.

Middleburg, J.J., C.H. Van-Der-Weijden and J.R.W. Woittiez, 1988. Chemical processes affecting the mobility of major, minor and trace elements during weathering of granitic rocks. Chem. Geol., 68: 253-273.

Moore, D.M. and R.C. Reynolds, 1989. X-Ray Diffraction and the Identification and Analysis of Clay Minerals. 1st Edn., Oxford University Press, Oxford New York, pp: 327-327.

Murry, H., 2007. Applied Clay Mineralogy Occurrences, Processing and Applications of Kaolins, Bentonites, Palygorskite-Sepiolite and Common Clays. 1st Edn., Elsevier, Oxford, New York, pp: 180-180.

Nesbitt, H.W., G. Markovics and R.C. Price, 1980. Chemical processes affecting alkalis and alkali earths during continental weathering. Geochim. Cosmochim. Acta, 44: 1659-1666.

Nesbitt, H.W. and G.M. Young, 1982. Early proterozoic climates and plate motions inferred from major element chemistry of lutites. Nature, 299: 715-717.

Nesbitt, H.W. and G.M. Young, 1996. Petrogenesis of sediments in the absence of chemical weathering: Effects of abrasion and sorting on bulk composition and mineralogy. Sedimentology, 43: 341-358.

Nesbitt, H.W., G.M. Young, S.M. McLennan and R.R. Keays, 1996. Effects of chemical weathering and sorting on the petrogenesis of siliciclastic sediments, with implications for provenance studies. J. Geol., 104: 525-542.

Picouet, C., B. Dupré, D. Orange and M. Valladon, 2002. Major and trace element geochemistry in the upper Niger river (Mali): Physical and chemical weathering rates and CO_2 consumption. Chem. Geol., 185: 93-124.

Reynolds, R.C., 1980. Interstratified Clay Minerals. In: Crystal Structures of Clay Minerals and their X-Ray Identification, Brindley, G.W. and Brown, G. (Eds.). Mineral Society, London, pp: 249-303.

Roddaz, M., J. Viers, S. Brusset, B. Baby, C. Boucayrand and G. Hérail, 2006. Controls on weathering and provenance in the Amazonian foreland basin: Insights from major and trace element geochemistry of Neogene Amazonian sediments. Chem. Geol., 226: 31-65.

Roser, B.P. and R.T. Korsch, 1988. Determination of tectonic setting of sandstone-mudstone suites using SiO_2 content and K_2O/Na_2O ratio. J. Geol., 94: 635-650.

Taraz, H., 1972. Geologic de la region surmag deh bid Iran central. These coc., Paris_sud Orsay.

Taylor, S.R. and S.M. McLennan, 1985. The Continental Crust: Its Composition and Evolution. Blackwell, Oxford: pp: 312.

Taylor, S.R. and S.H. McLennan, 1995. The geochemical evolution of the continental crust. Rev. Geophys., 33: 241-265.

Ugidos, J.M., Valladares, M.I. Barba and R.M. Ellam, 2003. The upper neoproterozoic-lower cambrian of the central Iberian zone, Spain: Chemical and isotopic (Sm-Nd) evidence that the sedimentary succession records an inverted stratigraphy of its source. Geochim. Cosmochim. Acta, 67: 2615-2629.

Weber, E.T., R.M. Owen, G.R. Dickens and D.K. Rea, 1998. Causes and implications of the middle rare earth element depletion in the eolian component of North Pacific sediment. Geochim. Cosmochim. Acta, 62: 1735-1744.

Wronkiewicz, D.J. and K.C. Condie, 1987. Geochemistry of archean shales from the witwatersrand supergroup, south Africa: Source-area weathering and provenance. Geochim. Cosmochim. Acta, 51: 2401-2416.

Wronkiewicz, D.J. and K.C. Condie, 1989. Geochemistry and provenance of sediments from the pongola supergroup, South Africa: Evidence for a 3.0 Ga old continental craton. Geochim. Cosmochim. Acta, 53: 1537-1549.

Wronkiewicz, D.J. and K.C. Condie, 1990. Geochemistry and mineralogy of sediments from the ventersdorp and transvaal supergroups, South Africa: Cratonic evolution during the early Proterozoic. Geochim. Cosmochim. Acta, 54: 343-354.